Correlating NQR transitions of ground and excited electronical states

Robert Klieber and Dieter Suter
Universität Dortmund, Fachbereich Physik, 44221 Dortmund, Germany
(Received 4 March 2005; published 24 June 2005)

Nuclear spins can be used as probes of electronic charge distribution by measuring frequencies of NMR transitions. Spins with $I>\frac{1}{2}$ are particularly sensitive to the charge distribution through the nuclear quadrupole coupling. While classical magnetic resonance experiments monitor only electronic ground states, it is possible to investigate also electronically excited states by using optical-radio frequency double resonance techniques. We use Raman heterodyne spectroscopy to directly correlate NMR transitions from an electronically excited state to the corresponding transitions in the electronic ground state of the same system in a time-resolved two-dimensional experiment.

DOI: 10.1103/PhysRevB.71.224418 PACS number(s): 76.30.Kg, 76.70.−r, 76.60.−k

I. INTRODUCTION

Among the main attractions of NMR is the possibility to use NMR spectra for obtaining information about electronic structure. The most important interactions that provide access to this information are the chemical shift and, for nuclei with spin $I>\frac{1}{2}$, the electric quadrupole interaction. Conventional magnetic resonance techniques obtain this information for electronic ground states, but if lasers are used to populate electronically excited states, chemical shift, and quadrupole couplings change, and NMR transitions get shifted. NMR spectra taken under such conditions thus allow one to probe electronically excited states.

An experimental technique that has proved particularly useful for studying electronically excited states is the Raman heterodyne technique (RHS).[1] It is based on coherent Raman scattering,[2,3] driven by a radio frequency magnetic field. A number of experiments[4–8] have demonstrated the potential of this technique for measuring NMR and nuclear quadrupole resonance (NQR) spectra from electronic ground state as well as electronically excited states. The analysis of the measured spectra allowed one to assign resonance lines to transitions between specific nuclear spin states.

If a material contains multiple nonequivalent sites in a unit cell, it is often possible to observe separate resonance lines for each site and study the change of electronic structure at each site separately. However, while it is usually possible to divide the observed spectra into subspectra associated with one site, the usual Raman-heterodyne spectra do not provide any information about which subspectrum of a given electronic state is associated with which subspectrum of another electronic state. It is therefore often not possible to determine how the change of electronic state affects a specific nuclear site.

A possible means to correlate different spectra involves the use of two-dimensional (2D) spectroscopy.[9,10] Here, we introduce a 2D experiment that directly correlates the spectra from two different electronic states. It involves frequency labeling of the transitions in one state, transfer of the populations between two electronic states, and detection in the second electronic state.

The paper is structured as follows. In the following section we give an overview of the relevant energy level scheme and the spectra of the individual electronic states. In Sec. III we describe the two-dimensional correlation experiment. Sections IV and V discuss experimental details and show experimental results from a representative system. The paper concludes with a summary of the main results.

II. SYSTEM AND ENERGY LEVELS

For the experiments we used a $Pr^{3+}:YAlO_3$ crystal, which has an orthorhombic unit cell containing two inequivalent praseodymium ion sites with a point symmetry C_{1h}.[11] Due to the low symmetry, all optical transitions between levels of the same $4f^N$ configuration are weakly allowed.[12] For these experiments, we use the transition between the $^3H_4$ and $^1D_2$ states. The excited state has a lifetime of $T_1=180\ \mu$s,[13,14] and in the absence of an external magnetic field, the optical transition has a dephasing time of $T_2=35\ \mu$s.[15,16]

The nuclear spin of ^{141}Pr $\left(I=\frac{5}{2}\right)$ can be described by the Hamiltonian

$$H = H_Q + H_Z, \tag{1}$$

where

$$H_Q = D\left[I_z^2 - \tfrac{1}{3}I(I+1)\right] + E(I_x^2 - I_y^2), \tag{2}$$

$$H_Z = -B_0\hbar(\gamma_x I_x \sin\theta\cos\phi + \gamma_y I_y \sin\theta\sin\phi + \gamma_z I_z\cos\theta). \tag{3}$$

The polar angles θ and ϕ describe the orientation of the static external magnetic field B_0 in the principal axis system of the ion's nuclear spins. Details about the quadrupole con-

TABLE I. Quadrupole parameters D and E, and gyromagnetic ratios of the $Pr^{3+}:YAlO_3$ Hamiltonian of the Pr^{3+} $^3H_4$ ground at 3 K and $^1D_2$ excited state at 12 K (see Refs. 17 and 18).

State	D (MHz)	E (MHz)	$\gamma_x/2\pi$ (kHz/G)	$\gamma_y/2\pi$ (kHz/G)	$\gamma_z/2\pi$ (kHz/G)
$^3H_4$	−3.5289	−0.0118	3.5	2.43	11.05
$^1D_2$	−0.4024	−0.0512	1.48	1.57	1.57

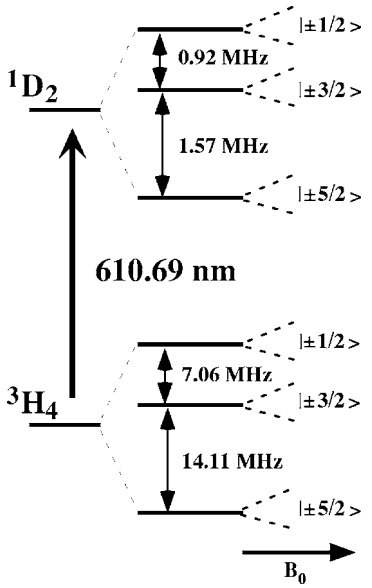

FIG. 1. Relevant part of the energy level scheme of $Pr^{3+}:YAlO_3$. Each electronic state consists of six nuclear spin substates, which are pairwise degenerate in the absence of a magnetic field.

stants (D,E) and the gyromagnetic ratios (γ_i) are shown in Table I. Due to the negative sign of the coupling constants, the states with $m_I=\pm\frac{5}{2}$ are the energetically lowest states.[7,8]

Figure 1 shows the relevant part of the energy-level scheme for the transition between $^3H_4$ and $^1D_2$ substates of $Pr^{3+}:YAlO_3$ for the case of a vanishing magnetic field.

A static magnetic field lifts the degeneracy of the nuclear spin states. Since the eigenstates of the Hamiltonian are not pure eigenstates of I_z, an alternating magnetic field can induce transitions between all nuclear spin states within a given electronic state. For a magnetic field of the order of 10 mT, e.g., the ground-state transition at 7 MHz splits into four transitions, corresponding to the nominal $\pm\frac{1}{2}\leftrightarrow\pm\frac{3}{2}$ transitions. Depending on the strength and orientation of the magnetic field, all four transitions can be (partly) allowed.

TABLE II. Orientation of the magnetic field in the principal axis systems of both sites and both electronic states.

State	Site	ϕ (°)	θ (°)
$^3H_4$	$1g$	90	68.4
	$2g$	90	44.4
$^1D_2$	$1e$	90	69.6
	$2e$	90	86.4

Since the praseodymium ions can occupy two nonequivalent sites in the $YAlO_3$ crystal, one observes a total of eight resonance lines in this frequency range.[5,17,19]

Figure 2 shows this spectrum for a magnetic field of 7.2 mT perpendicular to the crystal c axis. The spectrum was measured by Raman-heterodyne spectroscopy,[3] in a cw experiment. Since the transition matrix elements have different signs for the two sites, the resonance lines of one site have positive sign, while those originating from the other site have negative sign. We will refer to the site that gives positive resonance lines as site "1g," to that with negative lines as "2g." The inset of the figure indicates the individual transitions by numbers.

Figure 3 shows the corresponding spectrum from the electronically excited state. While these states are not populated at thermal equilibrium and the spectra therefore are not observable with conventional NMR/NQR techniques, they can be measured with the Raman heterodyne experiment.[1,4] Here we label the two sites with "1e" for the positive lines and "2e" for the negative lines. While the different signs of the resonance lines allow one to easily identify the resonance lines belonging to the same site within one electronic state, it is not possible to associate one set of resonance lines from the ground state with the corresponding set of resonance lines from the electronically excited state. The two possible assignments are $(1g=1e,\ 2g=2e)$ and $(1g=2e,\ 2g=1e)$.

III. CORRELATION EXPERIMENT

To correlate the transitions of the excited state with those of the ground state, we used a 2D time-domain experiment,

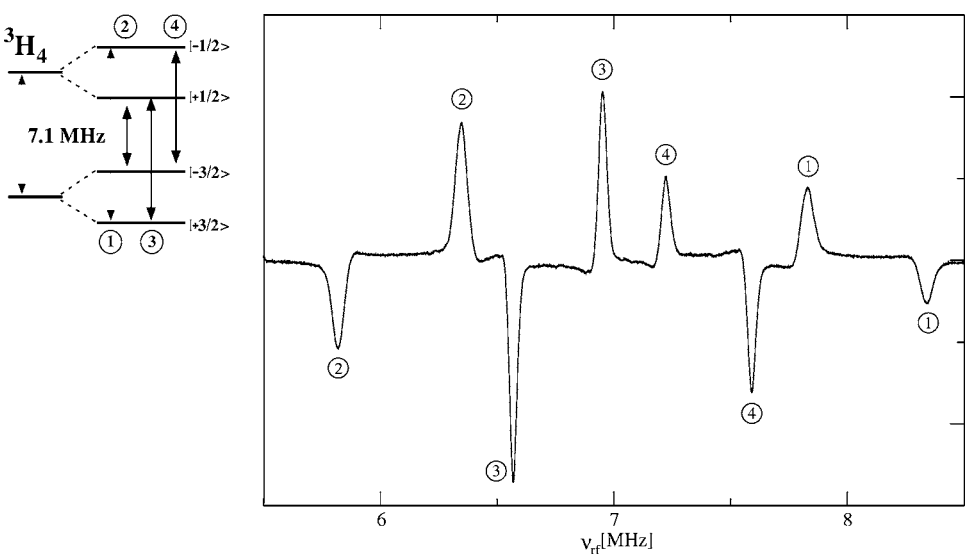

FIG. 2. Raman heterodyne spectrum for the $^3H_4\ |\pm\frac{1}{2}\rangle\leftrightarrow|\pm\frac{3}{2}\rangle$ transition of $Pr^{3+}:YAlO_3$ at 3 K. The external magnetic field for this configuraton is listed in Table II. Two inequivalent sites lead to eight transitions in the spectrum.

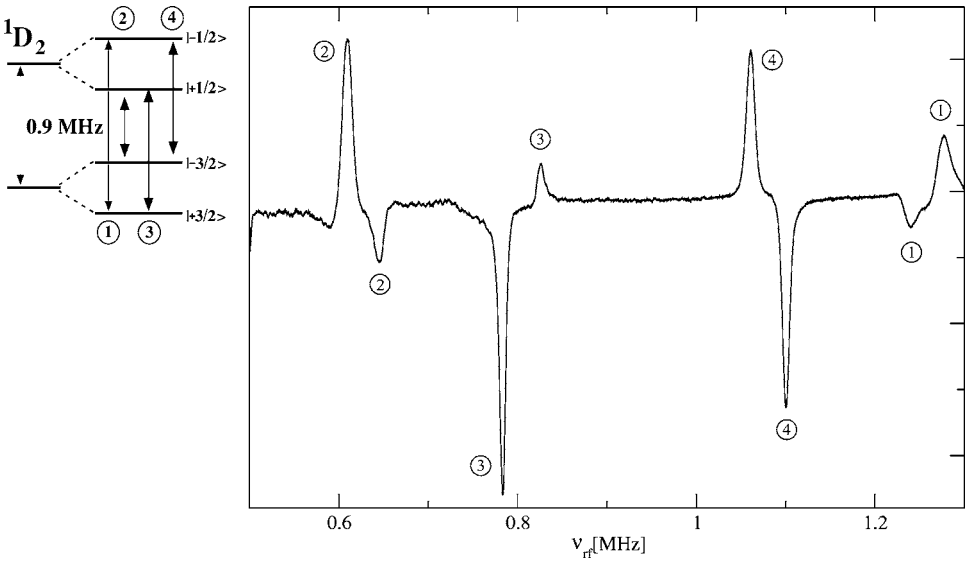

FIG. 3. Raman heterodyne spectrum for the $^1D_2\ |\pm\frac{1}{2}\rangle \leftrightarrow |\pm\frac{3}{2}\rangle$ transition of $Pr^{3+}:YAlO_3$ at 12 K. The external magnetic field is listed in Table II. Eight transitions can be found for two inequivalent sites.

where a signal $s(t_1,t_2)$ is recorded as a function of two independent time variables t_1 and t_2. We consider two nuclear spin states of the electronic ground state and two in the excited state and describe them as two pseudospin $\frac{1}{2}$ systems, which are connected by one optical transition.

Figure 4 illustrates the timing of the laser beam and the radio frequency fields for the correlation experiment. The pulses are assumed to be "hard" such that during the pulse any evolution of the state other than the action of the driving field is assumed to be negligible.

The initial laser pulse is a π pulse that transfers population from the ground to the excited state. We identify the excited state sublevel that is populated by the laser pulse with the $m_I=+\frac{1}{2}$ state of a pseudospin 1/2. After the laser pulse, the traceless part of the excited state density operator is thus proportional to

$$\rho_0 = S_z^e.$$

Here, S_z^e describes the z component of the virtual spin $\frac{1}{2}$ associated with the two spin sublevels of the electronically excited state. The density operator component proportional to the unity operator acting on the same subsystem can be neglected, since it is time independent and does not contribute to the signal.

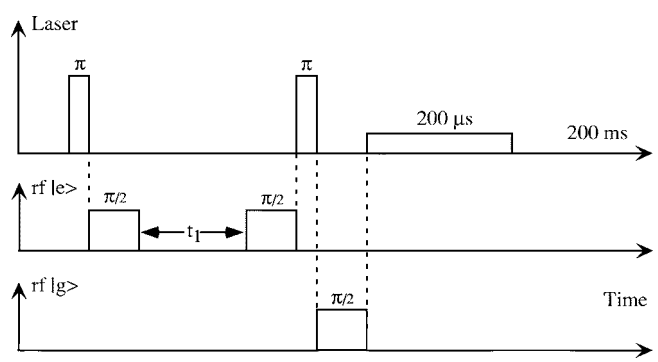

FIG. 4. Timing of the laser beam and the radio frequency fields. The top trace shows the laser pulses, the center trace the radio frequency pulses that are resonant with the excited state $m=\pm\frac{1}{2}\leftrightarrow\pm\frac{3}{2}$ transition, and the bottom trace the pulses that are resonant with the corresponding ground state transitions. The detection uses a weak laser pulse for Raman heterodyne detection of the ground state nuclear spin coherence.

A rf pulse that is resonant with the excited state NMR transition converts the population difference into coherence (transverse magnetization)

$$\rho_1 = e^{-i(\pi/2)S_x^e}\rho_0 e^{i(\pi/2)S_x^e} = -S_y^e.$$

This coherence evolves freely for a time t_1 to

$$\rho_2(t_1) = -S_y^e\cos(\omega_e t_1) + S_x^e\sin(\omega_e t_1).$$

Here, the precession frequency ω_e is given by the difference between the Zeeman frequency of the excited state nuclear spin and the applied rf frequency. A second $(\pi/2)_x$ rf pulse converts the y component into population difference

$$\rho_3 = -S_z^e\cos(\omega_e t_1).$$

We then use a second laser pulse to transfer the population from the excited state back to the electronic ground state. The relevant part of the ground state density operator thus becomes

$$\rho_4 = -S_z^g\cos(\omega_e t_1),$$

where we again neglect the component proportional to the unity operator of the ground state subsystem.

The ground state precession frequency is again measured in a rotating frame determined by the rf frequency. A radio frequency pulse that is resonant with the ground state nuclear spin transition converts this population difference into coherence within the $^3H_4$ electronic ground state, where it evolves during the detection time t_2. To observe the evolution of the coherence, we apply a weak laser pulse, which drives a coherent Raman process.[3] Phase-sensitive detection with the ground-state rf frequency yields the signal

$$s_1(t_1,t_2) = \cos(\omega_e t_1)e^{-i\omega_g t_2}.$$

A two-dimensional Fourier transform therefore yields a 2D spectrum, with the two frequency axes indicating the preces-

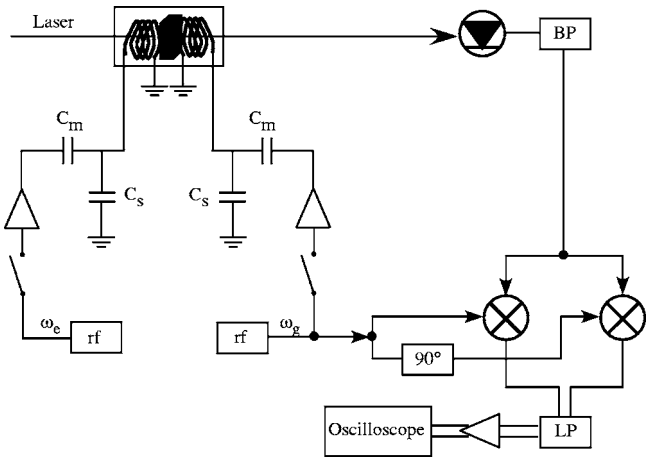

FIG. 5. Experimental setup: BP is a bandpass filter (3–10 MHz), LP is a lowpass filter (1.5 MHz), rf are the radio frequency generators producing the radio frequencies ω_g and ω_e, and 90° is a $\pi/2$ phase delay.

sion frequencies in the electronically excited state (ω_e) and in the electronic ground state (ω_g).

If the system contains two sites with different resonance frequencies, each of them gives rise to a separate line whose frequencies connect the ground state frequency to the corresponding excited state transition.

IV. EXPERIMENTAL SETUP

For the 2D-correlation experiment we used a $YAlO_3$ crystal with dimensions $5\times5\times1$ mm^3, in which 0.75% of the Y ions were substituted by praseodymium. The crystal was mounted on the cold finger of a helium flow cryostat and cooled to a temperature of 3 K. As shown in Fig. 5, the sample was excited with a laser beam tuned to the $^3H_4 \rightarrow {}^1D_2$ transition at 610.69 nm. The laser beam was produced by a tunable, actively stabilized ring dye laser (Coherent 899-21) and focused to a spot size of 100 μm in the sample. The laser frequency was swept linearly over 2 GHz within 25 s during the whole experiment to bring it into resonance with different ions in thermal equilibrium for subsequent shots. The laser beam propagated along the cristalographic c axis. The transmitted laser beam, together with the Raman field, was measured with a 200 MHz photodiode.

The laser beam excited the sample with a power density of 1.5 MW/m^2 for a pump pulse and 16 kW/m^2 for a detection pulse. The π-pulse length for an optical pump pulse was determined by a standard photon echo experiment and found to be 500 ns at 3 K. Since the optical dipole matrix elements are equal for the Z and Y directions of ions, the signals are independent of the laser polarization.[20]

The crystal was mounted between a pair of radio frequency coils. A single-tuned circuit was used for each coil with their resonance frequencies fixed near 6.62 and 1.09 MHz. The radio frequency fields, applied along the c axis, had an amplitude of approximately 28 G for the ground state and 65 G for the excited state, corresponding to a Rabi

TABLE III. Phase for the pulses in the excited state (e), in the ground state (g), and the demodulation phase used in the 2D-correlation experiment.

e	e	g	Demodulation
x	x	x	x
$\bar{x}$	x	$\bar{x}$	x
x	y	y	x
$\bar{x}$	y	$\bar{y}$	x

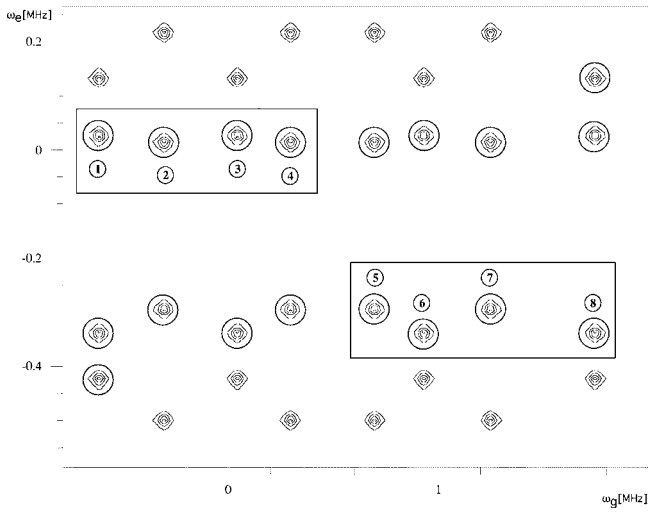

FIG. 6. 2D theoretical correlation spectrum for the $^1D_2$ 0.9 MHz and $^3H_4$ 7.1 MHz transition of Pr^{3+} in $YAlO_3$ at 3 K. The spectrum shows the first assignment described in the text correlating site 1g and 1e. Circled peaks were found in the experiments. Common peaks with the experimental spectra in Figs. 7 and 8 are numerized. The boxes indicate the frequency range covered by the experimental spectra of Figs. 7 and 8.

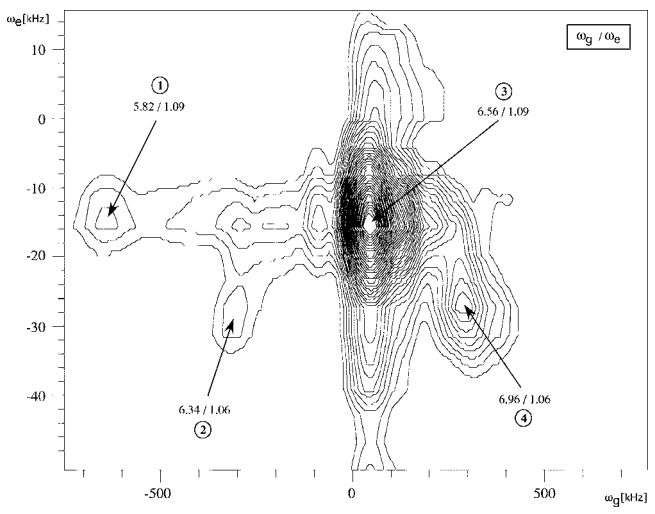

FIG. 7. Experimental correlation spectrum using rf 1.12 and 6.50 MHz for the excited and ground state, respectively. The numbering of the peaks is the same as in the theoretical spectrum of Fig. 6.

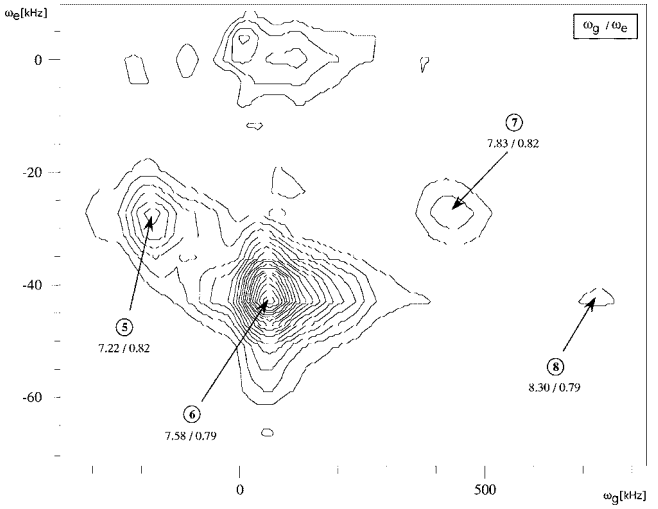

FIG. 8. Experimental correlation spectrum using rf 0.85 and 7.50 MHz for the excited and ground state, respectively. The numbering of the peaks is the same as in the theoretical spectrum of Fig. 6.

frequency of 100 kHz for the ground state transition at 6.62 MHz and 96 kHz for the excited state transition at 1.09 MHz, respectively, which was verified by pulsed Raman heterodyne experiments.

The Raman heterodyne signal was detected with a home-built photodetector and demodulated with the radio frequency that was used to excite the NQR transitions. After the signal was bandpass filtered and amplified, it was demodulated phase sensitive with ω_g and measured with a digital oscilloscope.

The correlation between the transitions in the ground and the electronically excited state can be determined by the pulse sequence described in Sec. III if the pulses are ideal. In practice, differences between transition matrix elements and off-resonance effects lead to unwanted signal contributions. To eliminate those, we used a four-step phase cycling scheme as summarized in Table III. For each t_1 increment, we added 4×80 scans.

V. RESULTS AND DISCUSSION

The experimental 2D-correlation spectrum is measured by increasing the time t_1 from 1 to 128 μs (Fig. 4). The FIDs are Fourier transformed according to the time axes t_1 and t_2. The resulting 2D spectrum shows the correlation between the ground and the excited state transitions. The horizontal axis illustrates the precession frequency ω_g for the ground and the vertical axis ω_e for the excited electronic state. The resonance lines in the 2D spectrum mark the frequency pairs ω_g, ω_e that are associated with one of the sites.

As discussed in the theoretical section, two possible combinations of ground state-excited state sites are possible. The eight ground state frequencies and eight excited state frequencies lead to 32 pairs of transition frequencies for each possible assignment. Figure 6 shows the resonance line positions that are expected for the combination ($1g=1e$, $2g=2e$).

Since it was not possible to excite the full spectral range of 3 MHz in the ground state and 0.8 MHz in the excited state with a single rf pulse, we measured a total of four experimental spectra, using different rf frequencies. Figures 7 and 8 show two of those spectra, identifying the relevant resonance lines. In the theoretical spectrum of Fig. 6, circles indicate which resonance lines were observed experimentally. Clearly, the experimental spectra support the assignment of site $1g$ with $1e$ and $2g=2e$.

VI. CONCLUSION

In conclusion, we proposed a method using pulsed Raman heterodyne technique to measure the correlation between transitions of two different electronic states in a two-dimensional correlation experiment and described it theoretically. We could distinguish between two possible site assignments for the ground state $^3H_4$ and the $^1D_2$ excited electronic state of $Pr:YAlO_3$. Most of the theoretical correlation peaks were found in the experiments and show, that the ground state site $1g$ and the excited state site $1e$ belong to a common site. This technique should be applicable to other systems as well, where more than one site exsists and Raman heterodyne signals are measurable.

ACKNOWLEDGMENT

This work was supported by the DFG through Grant No. Su 192/4-3.

[1] J. Mlynek, N. C. Wong, R. G. DeVoe, E. S. Kintzer, and R. G. Brewer, Phys. Rev. Lett. **50**, 993 (1983).
[2] E. Garmire, F. Pandarese, and C. H. Townes, Phys. Rev. Lett. **11**, 160 (1963).
[3] J. A. Giordmaine and W. Kaiser, Phys. Rev. **144**, 676 (1966).
[4] N. C. Wong, E. S. Kintzer, J. Mlynek, R. G. DeVoe, and R. G. Brewer, Phys. Rev. B **28**, 4993 (1983).
[5] M. Mitsunaga, E. S. Kintzer, and R. G. Brewer, Phys. Rev. Lett. **52**, 1484 (1984).
[6] L. E. Erickson, Phys. Rev. B **32**, 1 (1985).
[7] T. Blasberg and D. Suter, Phys. Rev. B **48**, 9524 (1993).
[8] R. Klieber, A. Michalowski, R. Neuhaus, and D. Suter, Phys. Rev. B **67**, 184103 (2003).
[9] A. A. Maudsley and R. R. Ernst, Chem. Phys. Lett. **50**, 368 (1977).
[10] J. Jeener, B. H. Meier, P. Bachmann, and R. R. Ernst, J. Chem. Phys. **71**, 4546 (1979).
[11] R. Diehl and G. Brandt, Mater. Res. Bull. **10**, 85 (1975).
[12] S. Hüfner, *Optical Spectra of Transparent Rare Earth Compounds* (Academic Press, New York, 1978).
[13] M. Mitsunaga, N. Uesugi, and K. Sugiyama, Opt. Lett. **18**, 1256 (1993).

[14] R. M. MacFarlane and R. M. Shelby, in *Spectroscopy of Solids Containing Rare Earth Ions*, edited by A. Kaplyanskii and R. M. MacFarlane (North-Holland, Amsterdam 1987).
[15] R. M. Shelby, R. M. Macfarlane, and R. L. Shoemaker, Phys. Rev. B **25**, 6578 (1982).
[16] R. M. Macfarlane, R. M. Shelby, and R. L. Shoemaker, Phys. Rev. Lett. **43**, 1726 (1979).
[17] M. Mitsunaga, E. S. Kintzer, and R. G. Brewer, Phys. Rev. B **31**, 6947 (1985).
[18] T. Blasberg and D. Suter, J. Lumin. **65**, 199 (1995).
[19] L. E. Erickson, Phys. Rev. B **42**, 3789 (1990).
[20] L. E. Erickson, Phys. Rev. B **19**, 4412 (1979).